Estimation of magnetosphere-ionosphere mapping accuracy using isotropy boundary and THEMIS observations

I. G. Shevchenko,[1] V. Sergeev,[1] M. Kubyshkina,[1] V. Angelopoulos,[2] K. H. Glassmeier,[3] and H. J. Singer[4]

Received 3 March 2010; revised 8 June 2010; accepted 23 July 2010; published 12 November 2010.

[1] It is difficult to establish the degree to which global magnetospheric mapping models are accurate, because there exists no definitive, independent method of validating such models. Toward that end we use the isotropy boundary (IB) of precipitation of energetic particles, as determined by low-altitude spacecraft. These particles are observed at ionospheric altitudes but their precipitation is governed by the magnetic field near the equator. Precipitating and trapped fluxes measured at the ionosphere can thus be used to determine the equatorial field strength, which can in turn be compared with predictions of magnetospheric models. By using hundreds of IB observations at the ionosphere during THEMIS major tail conjunctions in 2008 we report on the mapping accuracy obtained using three models: T96, AM-01, and AM-02. The first model is driven by the simultaneous solar wind and Dst measurements, whereas the latter two are obtained by fitting model data to THEMIS observations. The AM-02 and T96 models show comparable agreement with proton IB locations, with error estimates of about 1° in latitude. However, the AM-02 outperforms T96 in predicting electron IB locations. Mapping errors increase with magnetic activity and have significant magnetic local time dependence. We conclude that event-based magnetospheric models can be as good as or better than solar wind-based models, provided that a number of distributed magnetotail spacecraft are used to constrain model parameters.

Citation: Shevchenko, I. G., V. Sergeev, M. Kubyshkina, V. Angelopoulos, K. H. Glassmeier, and H. J. Singer (2010), Estimation of magnetosphere-ionosphere mapping accuracy using isotropy boundary and THEMIS observations, *J. Geophys. Res.*, *115*, A11206, doi:10.1029/2010JA015354.

1. Introduction

[2] The highly variable solar wind and complicated internal dynamics (e.g., substorms) of the Earth's magnetosphere make data-based magnetospheric modeling very difficult. The most widely used models are the empirical statistical models T89 and T96 [*Tsyganenko*, 1989, 1995], which models are constructed using hundreds of thousands of B vectors measured in the magnetosphere at different locations and under varying external conditions. In these models mathematical forms represent principal magnetospheric field sources treated as empirically defined functions of the solar wind and IMF parameters. The instantaneous magnetospheric configuration may deviate considerably from the average configuration represented by these standard models. Also, parameterizing the models using solar wind variables may be ambiguous in situations with a variable, inhomogeneous solar wind, because the data from a remote solar wind monitor may be quite inaccurate due to well-known difficulties in calculating time lags [*Weimer et al.*, 2002].

[3] An alternative approach intended to avoid these problems is based on an adaptive modeling technique which fits a model to the instantaneous magnetic field observed simultaneously by a number of magnetospheric spacecraft. Problems with this method include the limited amount of observational data and incomplete or uneven coverage of the localized region of interest. Previous attempts using this method have been mostly applied in the near tail region [e.g., *Pulkkinen et al.*, 1992; *Kubyshkina et al.*, 1999]. The mathematical framework used here was borrowed from the above-mentioned standard models, but some of the numerous parameters have been treated as variables to be determined by minimizing the model's standard deviation from the observed field.

[4] The THEMIS mission launched in 2007 includes a fleet of five equatorial spacecraft and a dense network of ground stations [*Angelopoulos*, 2008]. During the 3-month-

[1]Physics Faculty, St. Petersburg State University, St. Petersburg, Russia.
[2]Institute of Geophysics and Planetary Physics, University of California, Los Angeles, California, USA.
[3]Institut für Geophysik und Extraterrestrische Physik der Technischen Universität Braunschweig, Braunschweig, Germany.
[4]NOAA Space Weather Prediction Center, Boulder, Colorado, USA.

0148-0227/10/2010JA015354

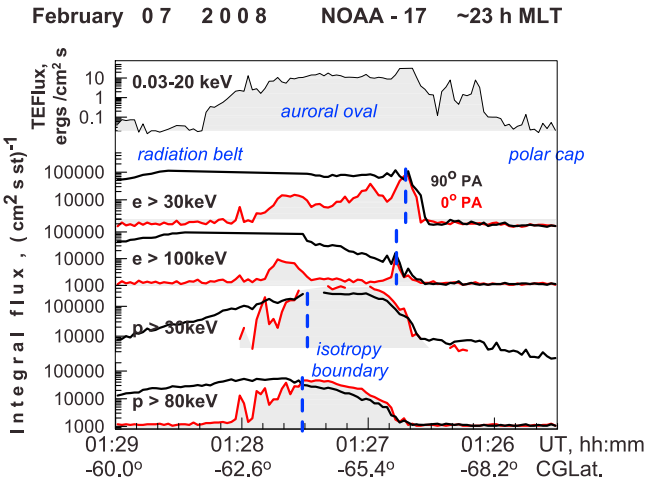

Figure 1. Example of auroral energy flux and integral energetic particle flux observations in different channels during traversal of the nightside auroral oval by the NOAA-17 spacecraft. Traces 0° and 90° pitch correspond to locally trapped particles and loss cone precipitation, respectively.

long magnetotail season, the THEMIS spacecraft, complemented by geosynchronous observations, repeatedly cover the middle magnetotail region from 6.6 to 30 R_E in the nightside magnetosphere, a great advantage for applying adaptive modeling. For this purpose a modified approach has been developed and two versions of data-based adaptive models (AM-01 and AM-02) have been constructed as described by *Kubyshkina et al.* [2009]. Comparison of these models with standard models and model error estimation are discussed in our paper.

[5] A part of this problem discussed here is the accuracy of magnetic mapping between the ionosphere and magnetosphere, which is especially important for THEMIS, whose major goal is to resolve the question of where the substorm arc maps in space and where the substorm onset region in the magnetosphere.

[6] In the past, magnetospheric model accuracy, particularly, mapping accuracy between the ionosphere and magnetosphere, could not be checked because of the lack of a reliable testing method. *Pulkkinen and Tsyganenko* [1996] tried to estimate the "internal" part of the mapping error in the T89 model by evaluating the vector difference between model field and magnetic field measurements (averaged in the vicinity of each point) when sliding along a magnetic field line. The absolute value of such errors was found to be largest on the dayside, while on the nightside the error was 0.5°–1.8° latitude at latitudes 63°–72°, increasing with geomagnetic activity. This approach evaluates only the part of the mapping error resulting from the data distribution and the quality of approximating functions in the basic models. It represents some average magnetosphere configuration and cannot characterize the mapping error in individual events.

[7] A quite different approach was investigated by *Weiss et al.* [1997], who used an independent mapping technique. They compared electron energy spectra at different points along DMSP spacecraft trajectories at low altitude with electron spectra measured simultaneously by nearly magnetically conjugate geosynchronous LANL spacecraft to identify when two spacecraft are on the same field line. Only initial results obtained with this technique have been published.

[8] During spacecraft traversal across the auroral zone, a sharp particle flux boundary was observed systematically by the low altitude spacecraft (see Figure 1). This "isotropy boundary" (IB) separates the (more poleward) region of isotropic precipitation from the (more equatorward) region with high trapped radiation belt flux but strongly suppressed particle flux precipitating in the loss cone center (at 0° pitch angles). This boundary is interpreted as a boundary between the (inner/outer) regions of adiabatic/stochastic particle motion in the equatorial magnetotail current sheet. This interpretation is supported by a specific rigidity-dependent ordering of the IB location (at lower latitude for higher rigidity $G = mv/q$, where m, v, and q are the mass, velocity, and charge of measured particles) and good correlation of the IB latitude with magnetic field inclination in the conjugate near-equatorial region [*Sergeev et al.*, 1983, 1993; *Newell et al.*, 1998]. Based on this interpretation, the IB latitude may be predicted by the magnetospheric model (after the critical point at the equator is found and mapped along the magnetic field line into the ionosphere) using a $R_c/\rho = B_n^2/(G\partial B_t/\partial n) \sim 8$, where n and t denote the normal and tangential directions with respect to the current sheet [*Sergeev et al.*, 1993; *Donovan et al.*, 2003; *Lvova et al.*, 2005]. Produced in the near-equatorial region and controlled (and predicted) by the magnetic field in that region, low-altitude observations of isotropy boundaries carry information about field-line mapping and therefore provide a suitable tool to probe the mapping accuracy of magnetospheric models.

[9] In this paper we describe how this technique can be used and apply it to evaluate statistically the mapping accuracy of three magnetospheric models, the standard T96 model using solar wind parameters and two data-based models adapted to simultaneous magnetotail observations made by the five THEMIS spacecraft.

2. Models and Observations

[10] In this paper we investigate three magnetospheric models. The widely used standard T96 model [*Tsyganenko*, 1995] allows us to compute the magnetic field at a specified point inside the magnetosphere for the specified epoch providing four external parameters (the solar wind dynamic pressure Pd, B_z, and B_y IMF components, and D_{st} index) are known. We used the time-shifted 5 min averaged OMNI parameters to run the T96 model.

[11] The procedure to construct the two time-dependent adapted models AM-01 and AM-02 was described in detail in *Kubyshkina et al.* [2009] (hereafter referred to as Paper 1). Although these models borrow functional forms from the T96 model, four external parameters are obtained by best fit of the model to the observations made simultaneously by several (basically THEMIS) spacecraft. With the exception of the AM-02, which allows the neutral sheet tilt in the GSM XZ plane to be varied, the models leave internal model parameters intact. Rather than being taken from solar wind observations, the four external parameters of the T96 models are

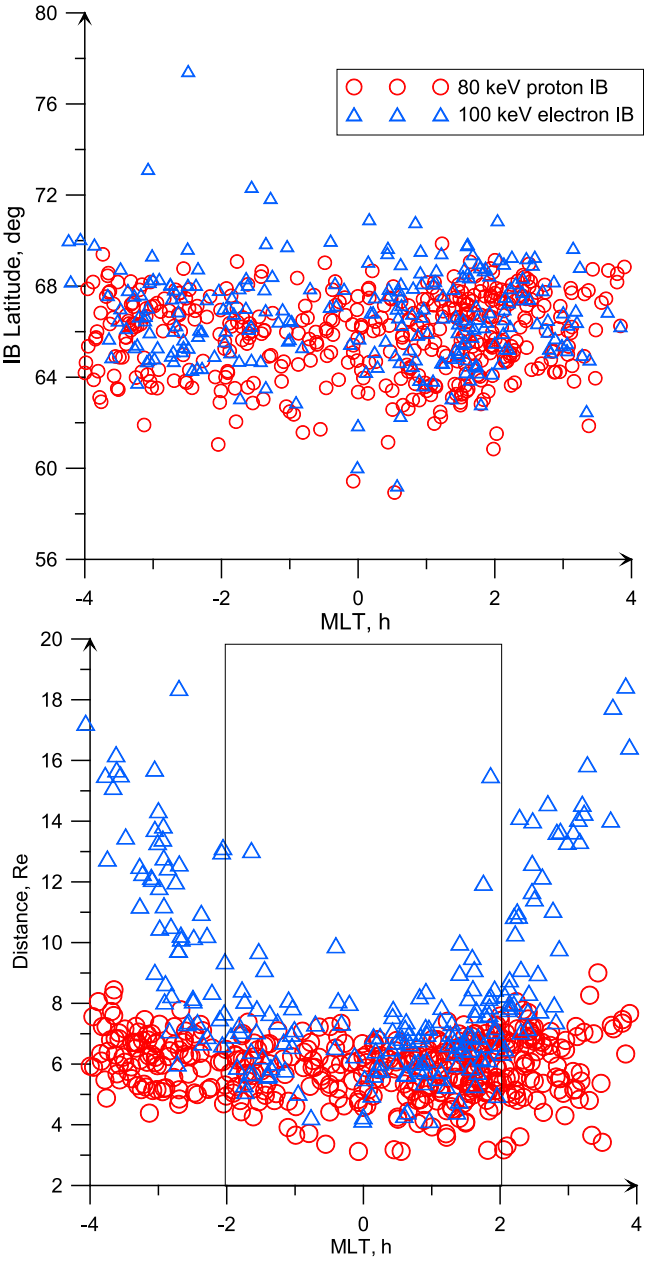

Figure 2. Distribution of observed isotropy boundaries in (top) CGLatitude-MLT coordinates and (bottom) corresponding points in the magnetic equatorial plane mapped using the AM-02 model. MLT refers to the ionospheric foot point of the corresponding magnetic field line. ProtonIBs and electron IBs are shown by red circles and blue triangles, respectively.

treated as variables the values of which are found by minimizing the fit function F:

$$F = \frac{\sqrt{\sum_{i=1}^{N}\sum_{j=1}^{3}\left(B_{ij}-B'_{ij}\right)^2}}{\sum_{i=1}^{N} W_i} + \frac{\sum_{m=1}^{M}\left(\sqrt{B^2_{\mathrm{tot}_m}} - \sqrt{P_{\mathrm{tot}_m}\times 2\mu_0}\right)}{\sum_{m=1}^{M} W^i_m},$$

where B_{ij} is the magnetic field j-th component measured at i-th spacecraft, B'_{ij} is the model magnetic field j-th component at i-th spacecraft location, M is the the number of distant spacecraft (situated at $r > 15\ R_E$ in the magnetotail), and N is the the total number of spacecraft used. W_i stands for the weighting coefficient of i-th spacecraft depending on its position relative to magnetopause, Earth, and other spacecraft. W^i_m is the weighting factor which is defined by whether a spacecraft is distant (see Paper 1 for details). We use only the first term in the fit function and magnetic data from the five THEMIS spacecraft to fit the AM-01 model. In the AM-02 model we use both terms and include additional measurements when available. In addition to plasma pressure data from two distant THEMIS spacecraft (P1 and P2), we use available magnetic observations made by the Geostationary Operational Environmental Satellite 11 (GOES-11) and GOES-12 spacecraft in the nightside portion of their geostationary orbit. The control of total (plasma plus magnetic) pressure is important to limit the total magnetotail current (Paper 1).

[12] For this study we selected 9 days from the 2008 THEMIS magnetotail season (January–March), including 8 days of major conjunctions and one minor conjunction day. Particle observations made by five National Oceanic and Atmospheric Administration (NOAA) polar-orbiting spacecraft on these days were processed to determine the equatorward most limit of the isotropic particle distributions and define the corrected geomagnetic latitude (IBLat) and magnetic local time (MLT) corresponding to the isotropy boundary. This was carried out by comparing the energetic particle fluxes measured in the downward radial and transverse direction (0° and 90° pitch angles as shown in Figure 1). We used the measurements from the >80 keV proton channel and >100 keV electron channel of the MEPED instruments (see for reference *Evans and Greer*, 2006).

[13] It is known that IB latitude has a pronounced daily variation (going nearly along the auroral oval) and that IBLat (MLT) function has a plateau region on the nightside (see, e.g., *Lvova et al.* [2005]). Although the distribution of measured IB latitudes within 4 h MLT around magnetic midnight shown in Figure 2 (top) confirms this, it also shows that electron boundaries still have substantial average IBLat (MLT) variations. Considering that the error in the region of large IBLat (MLT) gradients will potentially increase, for our purposes (mapping error evaluation) we restricted the MLT region where the electron IB data are analyzed to be within 2 h MLT of the magnetic midnight. Finally we selected about 440 events for the 80 keV proton IB and about 200 events for the 100 keV electron IB observations to perform the mapping error estimation. For this purpose, in each case we computed the model prediction for both ion and electron IBs at the meridian of the isotropy boundary observation for all three models. The AM-01 and AM-02 models are available at 5 min steps (Paper 1) so the time difference between the model epoch and the IB observation time does not exceed 5 min. Figure 2 (bottom) shows the distribution of isotropic boundaries mapped into the ionosphere using the AM-02 model illustrating which region is actually investigated. The proton isotropy boundaries cover the region in the nightside magnetosphere within 2 R_E of geostationary orbit, whereas the electron boundaries cover mostly the outer part of the inner magnetosphere, within 10 Re, with very few points

Table 1. Average Mapping Error, Standard Deviation Between Predicted and Observed Isotropy Boundaries, and Their Correlation Coefficient

	T96			AM-01			AM-02		
	Error $\langle\lvert\Delta\Lambda\rvert\rangle$	SD	CC	Error $\langle\lvert\Delta\Lambda\rvert\rangle$	SD	CC	Error $\langle\lvert\Delta\Lambda\rvert\rangle$	SD	CC
Protons	1.01	0.65	0.79	1.87	1.41	0.66	1.01	0.73	0.85
Electrons (|MLT| < 2)	2.07	1.11	0.44	2.23	1.56	0.47	1.57	1.09	0.58

mapped to farther distances, and these are mostly at MLT < 22 h and MLT > 02 h.

3. Error Estimation Results

[14] In the following, "mapping error" means the absolute value of the difference between the measured IB latitude and the IB latitude predicted by the model. And by MLT of the IB we mean MLT of the ionospheric point. The quantitative results characterizing the mapping errors and correspondence between predicted and observed IBs including the average mapping error ($\Delta\Lambda$), standard deviation between predicted and observed isotropy boundaries (SD) and their correlation coefficient (CC) are collected in Table 1. The scatter of data points, with all ordinate axes in the same range from 56° to 74° to facilitate comparisons, can be seen in Figure 3. Figure 4 helps to characterize the activity dependence. The three different models are shown in these plots (from left to right: T96, AM-01, and AM-02).

[15] Table 1 and Figures 3 and 4 clearly show that the three models tested differ in the quality of their prediction. There is also a difference between results for protons and electrons. In Figure 3, the proton data points form dense distributions with regression lines close to the diagonal (shown in red) (the standard deviation of the best models is about 0.7°). The electron predictions are less accurate (their standard deviation is about 1.1°). Of the three models, AM-01 shows the worst result, which is consistent with the analysis in Paper 1. Figure 3 shows that the AM-01 model seriously underestimates the IB latitude for low latitudes (below 65°), that is for active conditions for protons. According to Paper 1, the main reason is that this model (simplest) can only react to decreasing current sheet thickness by increasing the magnetotail current. In comparison, the AM-02 model has more flexibility. It sustains the total current by means of the total pressure term in the fit function (F). It also includes a variable current sheet tilt to simulate the neutral sheet positional changes.

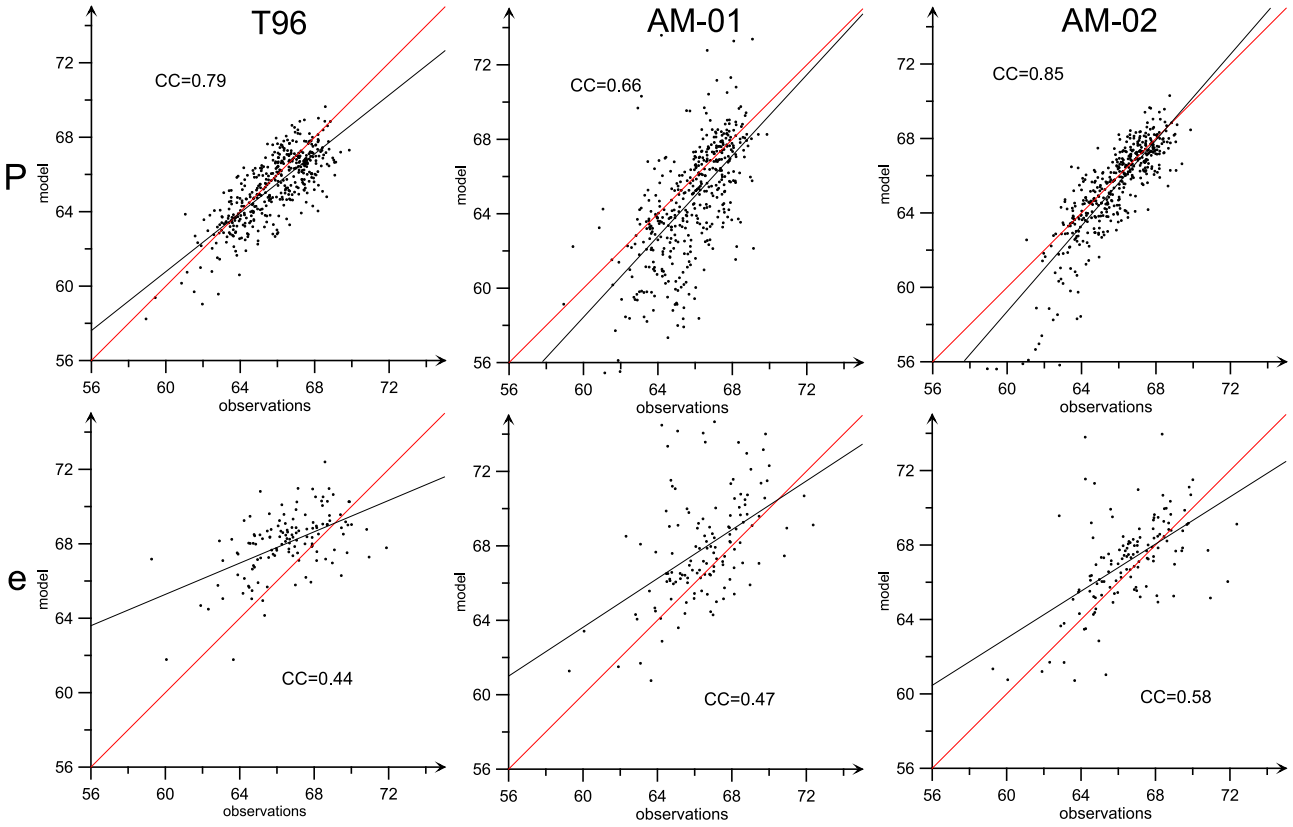

Figure 3. Comparison of modeled and observed IB latitudes for the entire data set. (top) Proton IB data, and (bottom) electron IB data. Figures 3 (left), 3 (middle), and 3 (right) correspond to the three different models. Correlation coefficients (CC) and linear regression (black lines) are also shown for each plot.

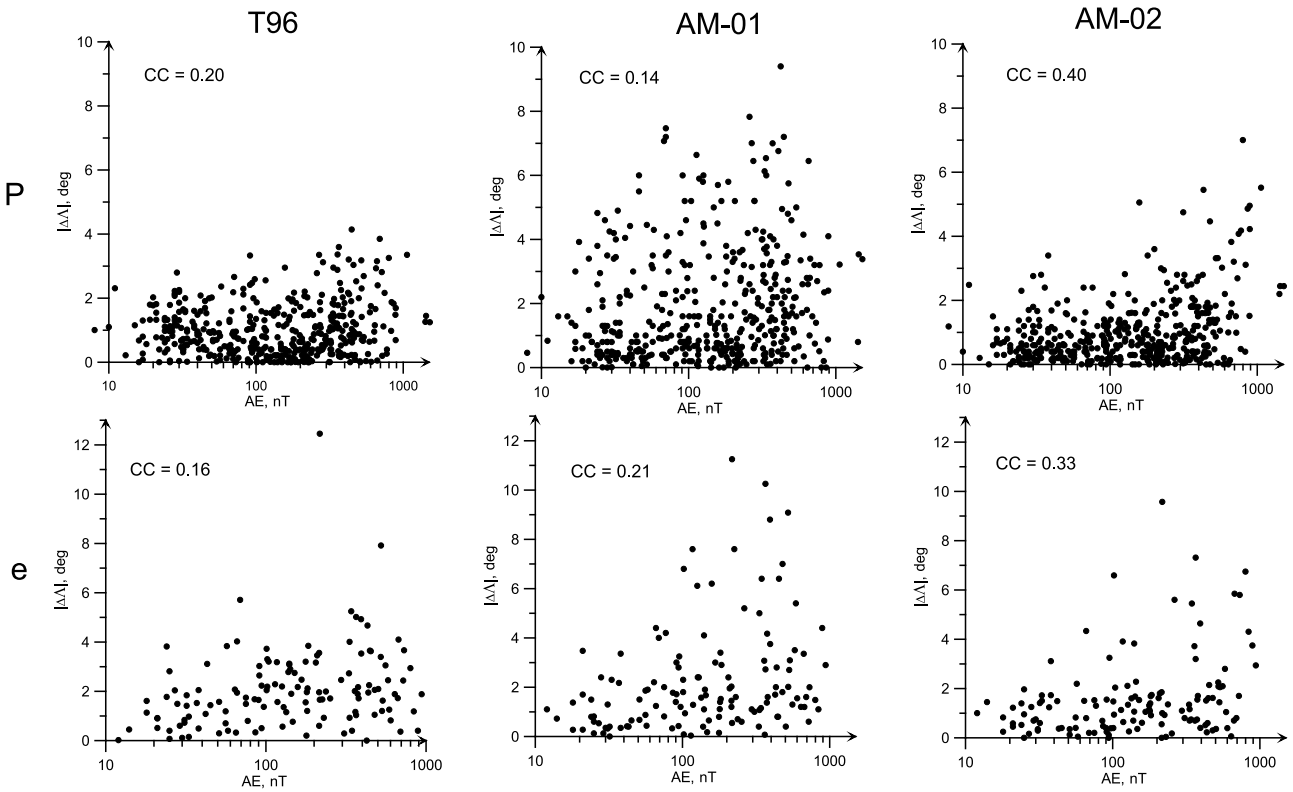

Figure 4. Dependence of mapping error on the AE index. (top) Proton IB data, and (bottom) electron IB data. Figures 4 (left), 4 (middle), and 4 (right) correspond to the three different models. Correlation coefficients (CC) are also shown for each plot.

[16] Although correlation between the mapping error and AE was found to be quite small (CC ranges between 0.1 and 0.4) activity dependence clearly exists. In the plots we see that at the low activity end all data points are clustered within 2° of zero, and the standard deviation is always small. With increasing activity, however, the upper envelope of the data point cloud also increases (this is best seen in AM-02 plots). At the same time there still exist many data points with small errors at the high activity end, which explain the resulting low correlation coefficient. To understand such scatter we must remember that during active conditions two different types of deviation from the "average model" occur: one corresponds to strong magnetotail stretching and formation of the thin current sheet (e.g., the growth phase) and the other to relaxed dipolarized configuration (during the expansion/recovery phase).

[17] The quality of the model representation may vary with magnetic local time. We check this by plotting the mapping errors against MLT in Figure 5 (here we use different symbols for different magnetic activity ranges). Results show no strong dependence for the best-performing models T96 and AM-02. Yet, a weak positive slope in the IBLat (MLT) cloud of points can be discerned. This dependence may be understood as an effect of the partial ring current which provides a B_z depression (and a more Earthward IB location in the magnetosphere) on the dusk side but that is absent in the T96, AM-01, and AM-02 models.

[18] The mapping error examined above may include details of the isotropy boundary which are not expected to be predicted by the magnetospheric models. For example, processes other than nonadiabatic particle scattering in the current sheet (e.g., wave-particle interactions intensified during storms or inside the dipolarized region) can sometimes contribute to boundary formation. Also, in the presence of longitudinally localized meso-scale structures in the current system (which are absent in standard and adapted models) the IB latitude may vary with longitude. This part can be estimated experimentally by comparing nearly simultaneous (within 10 min) isotropy boundary crossings of two NOAA spacecraft at nearly the same MLT (within 1 h MLT). In our data set we found 40 such events in proton data and 14 in electron observations. The average latitudinal difference between two IB determinations was found to be $0.47 \pm 0.36°$ for proton IB and $0.45 \pm 0.33°$ for electron IB. These values are a significant part (up to a half) of the average mapping errors given in Table 1. Therefore, the real accuracy of the mapping can be better than that characterized by the values given in Table 1, which have to be considered as upper bound of real accuracy.

4. Discussion and Concluding Remarks

[19] The main problem with estimation of mapping accuracy is that the actual magnetic configuration (for which the magnetospheric models provides an approximation) is unknown, and independent reliable mapping tools (not relying exclusively on magnetospheric models) are not available. The suggestion to use the isotropy boundary observations to characterize the magnetic field configuration seems rather natural, considering the previous demonstrations of the close

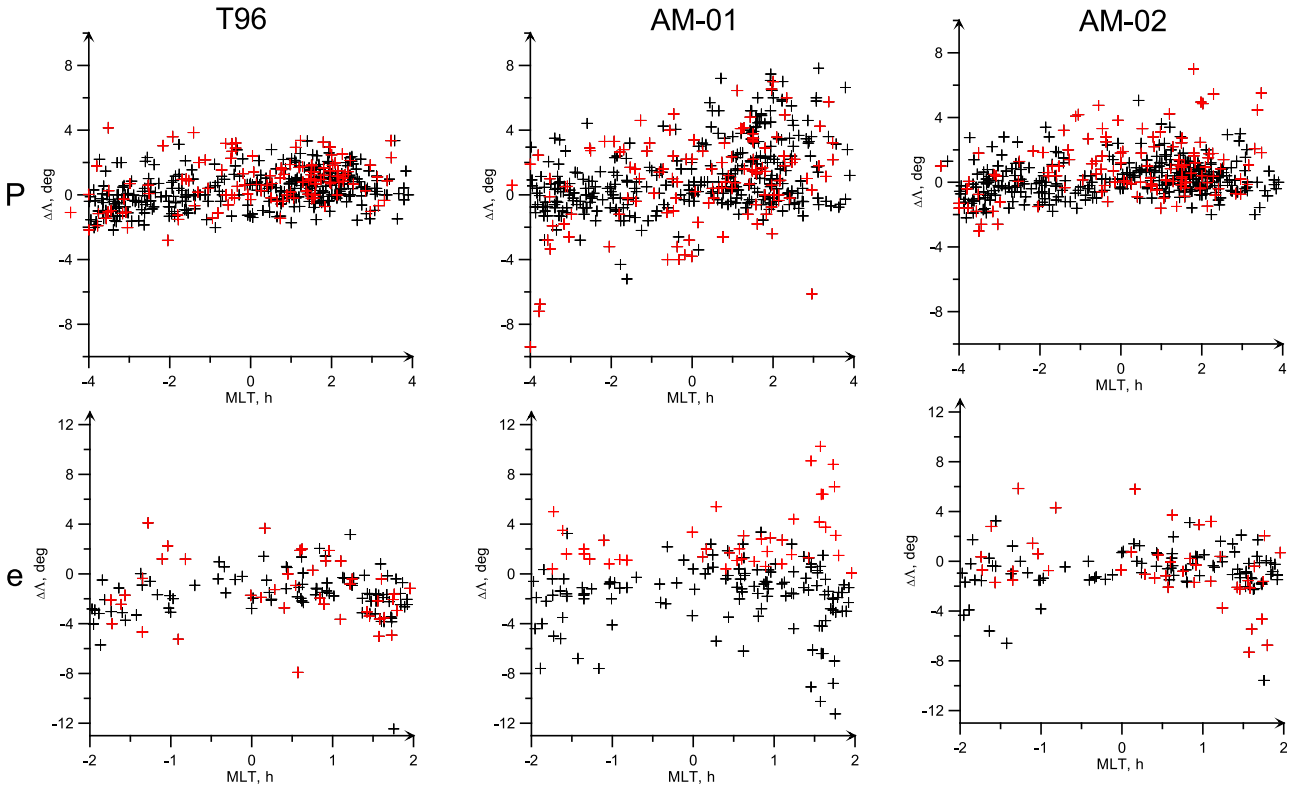

Figure 5. Dependence of the mapping error on MLT. (top) Proton IB data, and (bottom) electron IB data. Figures 5 (left), 5 (middle), and 5 (right) correspond to the three different models. Red crosses indicate events during active time (AE > 300).

relation between the IB and magnetic field stretching in the magnetotail [*Sergeev et al.*, 1993; *Newell et al.*, 1998; *Donovan et al.*, 2003, etc.], as well as good documentation of its use in practice to categorize quantitatively magnetic field stretching or to select an appropriate model [*Kubyshkina et al.*, 1999; *Wing and Newell*, 1998; *Sotirelis and Newell*, 2000]. Vice versa, small deviations of IB observations from its predictions made by the best data-based adapted time-dependent magnetospheric model (AM-02) once again demonstrate its predictive power to evaluate the magnetospheric configuration.

[20] In this paper we evaluated the accuracy of the mapping procedure for three models using IB observations. We found an average mapping error value of 1° for the standard T96 and AM-02 models and about 1.8° for AM-01 (when using proton IB). The mapping errors obtained using electron IB are 2.07° (T96), 2.23° (AM-01), and 1.57° (AM-02). The mapping error increases with magnetic activity in that its upper envelope is increasing (although a large percentage of crossings still show a small mapping errors). These numbers characterize the mapping error in the near tail region between geostationary orbit and a circle at ~10 R_E. We also compared the IB determinations when two spacecraft crossed the same part of the auroral oval almost simultaneously and found latitudinal differences roughly ~0.5°. This is nearly a half of the statistical mapping error found in our analyses and represents the upper bound of mapping accuracy.

[21] When comparing quantitatively our evaluation of mapping accuracy with two previous investigations [*Pulkkinen and Tsyganenko*, 1996; *Weiss et al.*, 1997], one must keep in mind that they both investigated the T89 model which is parametrized by the Kp index and has a coarse (3 h) time resolution, whereas we dealt with the more refined T96 model and its adaptive modifications.

[22] *Pulkkinen and Tsyganenko* [1996] integrated the vector difference between the model field and magnetic field measurements, averaged in the vicinity of points along magnetic field line. They covered all MLTs at magnetic latitudes above 63° for different Kp index ranges. In their analyses, the absolute value of the mapping error was about a 0.5° in the nightside auroral oval when Kp = 0; this value increased to 1.8° when Kp = 5. These numbers are similar to or larger in magnitude than ours, which are on the order of ~1°. Recalling that the principal deficiency of this approach is that it only provides a statistical accuracy estimation (it characterizes the statistical distribution in the observational data subset, ordered by Kp and the quality of interpolation), it cannot be used for mapping accuracy estimation for a single event.

[23] *Weiss et al.* [1997] used an independent mapping technique based on closest matching of electron energy spectra observed simultaneously by geosynchronous spacecraft and low-altitude DMSP spacecraft that crossed the auroral zone at the same meridian. They focused on another problem (the best indices to characterize magnetic field line stretching), used a relatively small number of analyzed conjugate events on the nightside (~40) and did not provide statistical information about mapping accuracy. From their Figure 4, however, we can determine that the median latitudinal difference between actual mapping and the T89 pre-

diction is about 2° (maximal deviation as large as 9°). This error is twice as large as our median error for proton IB, which is understandable considering that we use the improved model (T96 rather than T89) and run it at 5 min time resolution (rather than the 3 h resolution of the Kp index).

[24] To summarize, we tested a new method to evaluate the accuracy of field-line mapping using isotropy boundary observations made by low-altitude spacecraft. The method performs quite well and may be an easy way of testing models in standard conditions (expanding it to storm conditions requires a special study). With this tool we demonstrated the statistical quantitative estimate of the mapping accuracy in the nightside magnetotail at distances between (roughly) 6 and 10 R_E appeared to be better than 1°. Comparison with previous accuracy estimates indicates that both T96 and the AM-02 adaptive models perform a better mapping and are better models than T89. An encouraging fact is that the AM-02 model gives the same or better results than the T96 standard model, implying that we may use the adaptive model for accurate mapping in the situation when solar wind data are unavailable of or when it is difficult to accurately time shift solar wind observations from interplanetary spacecraft to the Earth's magnetopause.

[25] **Acknowledgments.** Energetic particle observations from NOAA-POES spacecraft (D. Evans, PI) are made available by NOAA and OMNI interplanetary data are available via http://omniweb.gsfc.nasa.gov. We acknowledge NASA contracts NNX08AD85G and NAS5-02099, the German Ministry for Economy and Technology and the German Center for Aviation and Space (DLR), contract 50 OC 0302. The work by I.S., V.S., and M.K. was supported by the Russian Ministry of Education and Science grants, by CRDF grant RUG1-2861-ST-07, by RFBR grants 10-05-91163 and 10-05-00223, and by EUgrant 263325. We thank M. Holeva and Judy Hohl for help with preparation of this paper.

[26] Masaki Fujimoto thanks Joachim Vogt and another reviewer for their assistance in evaluating this paper.

References

Angelopoulos, V. (2008), The THEMIS mission, *Space Sci. Rev.*, *141*, doi:10.1007/s11214-008-9336-1.

Auster, H. U., et al. (2008), The THEMIS fluxgate magnetometer, *Space Sci. Rev.*, *141*, 235–264, doi:10.1007/s11214-008-9365-9.

Delcourt, D. C., J.-A. Sauvaud, R. F. Martin Jr., and T. E. Moore (1996), On the nonadiabatic precipitation of ions from the near-Earth plasma sheet, *J. Geophys. Res.*, *101*(A8), 17,409–17,418.

Donovan, E. F., B. J. Jackel, I. Voronkov, T. Sotirelis, F. Creutzberg, and N. A. Nicholson (2003), Ground-based optical determination of the b2i boundary: A basis for an optical MT-index, *J. Geophys. Res.*, *108*(A3), 1115, doi:10.1029/2001JA009198.

Evans, D. S., and M. S. Greer (2006), *Polar Orbiting Satellite Space Environment Monitor-2: Instrument Descriptions and Archive Data Documentation*, NOAA, Washington, D.C.

Kubyshkina, M. V., V. A. Sergeev, and T. I. Pulkkinen (1999), Hybrid input algorithm: An event-oriented magnetospheric model, *J. Geophys. Res.*, *104*(A11), 24,977–24,993.

Kubyshkina, M. V., V. A. Sergeev, N. Tsyganenko, V. Angelopoulos, A. Runov, H. Singer, K. H. Glassmeier, H. U. Auster, and W. Baumjohann (2009), Toward adapted time-dependent magnetospheric models: A simple approach based on tuning the standard model, *J. Geophys. Res.*, *114*, A00C21, doi:10.1029/2008JA013547.

Lvova, E. A., V. A. Sergeev, and G. R. Bagautdinova (2005), Statistical study of the proton isotropy boundary, *Ann. Geophys.*, *23*, 1311–1316.

Newell, P. T., V. A. Sergeev, G. R. Bikkuzina, and S. Wing (1998), Characterizing the state of the magnetosphere: Testing the ion precipitation maxima latitude (b2i) and the ionisotropy boundary, *J. Geophys. Res.*, *103*(A3), 4739–4745.

Pulkkinen, T. I., D. N. Baker, R. J. Pellinen, J. Büchner, H. E. J. Koskinen, R. E. Lopez, R. L. Dyson, and L. A. Frank (1992), Particle scattering and current sheet stability in the geomagnetic tail during the substorm growth phase, *J. Geophys. Res.*, *97*(A12), 19,283–19,297.

Pulkkinen, T. I., and N. A. Tsyganenko (1996), Testing the accuracy of magnetospheric model field line mapping, *J. Geophys. Res.*, *101*(A12), 27,431–27,442.

Sergeev, V. A., E. M. Sazhina, N. A. Tsyganenko, J. A. Lundblad, and F. Soraas (1983), Pitch-angle scattering of energetic protons in the magnetotail current sheet as the dominant source of their isotropic precipitation into nightside ionosphere, *Planet. Space Sci.*, *31*, 1147–1158.

Sergeev, V. A., M. Malkov, and K. Mursula (1993), Testing the isotropic boundary algorythm method to evaluate the magnetic field configuration in the tail, *J. Geophys. Res.*, *98*(A5), 7609–7620, doi:10.1029/92JA02587.

Sotirelis, T., and P. T. Newell (2000), Boundary-oriented electron precipitation model, *J. Geophys. Res.*, *105*(A8), 18,655–18,673.

Tsyganenko, N. A. (1989), Magnetospheric magnetic field model with a warped tail current sheet, *Planet. Space Sci.*, *37*, 5.

Tsyganenko, N. A. (1995), Modeling the Earth's magnetospheric magnetic field confined within a realistic magnetopause, *J. Geophys. Res.*, *100*(A4), 5599–5612.

Weimer, D. R., D. M. Ober, N. C. Maynard, W. J. Burke, M. R. Collier, D. J. McComas, N. F. Ness, and C. W. Smith (2002), Variable time delays in the propagation of the interplanetary magnetic field, *J. Geophys. Res.*, *107*(A8), 1210, doi:10.1029/2001JA009102.

Weiss, L. A., M. F. Thomsen, G. D. Reeves, and D. J. McComas (1997), An examination of the Tsyganenko (T89a) field model using a database of two-satellite magnetic conjunctions, *J. Geophys. Res.*, *102*(A3), 4911–4918.

Wing, S., and P. Newell (1998), Central plasma sheet ion properties as inferred from ionospheric observations, *J. Geophys. Res.*, *103*(A4), 6785–6800.

V. Angelopoulos, Institute of Geophysics and Planetary Physics, University of California, Los Angeles, CA 90095, USA.

K. H. Glassmeier, Institut für Geophysik und Extraterrestrische Physik der Technischen Universität Braunschweig, Mendelssohnstraße 3, D-38106 Braunschweig, Germany.

M. V. Kubyshkina, V. A. Sergeev, and I. G. Shevchenko, Physics Faculty, St. Petersburg State University, St. Petersburg 198504, Russia. (i.g.shevchenko@gmail.com)

H. J. Singer, NOAA Space Weather Prediction Center, Boulder, CO 80305, USA.